8042–8051 *Nucleic Acids Research, 2011, Vol. 39, No. 18* *Published online 30 June 2011*
doi:10.1093/nar/gkr502

DNA cleavage site selection by Type III restriction enzymes provides evidence for head-on protein collisions following 1D bidirectional motion

Friedrich W. Schwarz[1], Kara van Aelst[2], Júlia Tóth[2], Ralf Seidel[1,*] and Mark D. Szczelkun[2,*]

[1]Biotechnology Center, Dresden University of Technology, 01062 Dresden, Germany and [2]DNA-Protein Interactions Unit, School of Biochemistry, Medical Sciences Building, University of Bristol, Bristol, BS8 1TD, UK

Received April 8, 2011; Revised May 27, 2011; Accepted June 2, 2011

ABSTRACT

DNA cleavage by the Type III Restriction–Modification enzymes requires communication in 1D between two distant indirectly-repeated recognitions sites, yet results in non-specific dsDNA cleavage close to only one of the two sites. To test a recently proposed ATP-triggered DNA sliding model, we addressed why one site is selected over another during cleavage. We examined the relative cleavage of a pair of identical sites on DNA substrates with different distances to a free or protein blocked end, and on a DNA substrate using different relative concentrations of protein. Under these conditions a bias can be induced in the cleavage of one site over the other. Monte-Carlo simulations based on the sliding model reproduce the experimentally observed behaviour. This suggests that cleavage site selection simply reflects the dynamics of the preceding stochastic enzyme events that are consistent with bidirectional motion in 1D and DNA cleavage following head-on protein collision.

Type III restriction endonucleases (REs) will cut DNA molecules in an ATP-dependent manner when there are two copies of the cognate asymmetric recognition site in an inverted repeat arrangement (1–5). These sites can be many thousands of base pairs apart, but must be on the same DNA chain (6). Whilst sites in either head-to-head (HtH) or tail-to-tail (TtT) orientation can efficiently induce the nuclease activity, DNA with single sites or with pairs of sites in direct (head-to-tail, HtT) repeat do not, except under conditions which promote non-specific association with the DNA (e.g. K^+ ions and/or elevated enzyme concentrations) (4,7). The Type III REs can therefore be said to exhibit 'site orientation selectivity' (1,5). This selectivity is important since these enzymes only hemimethylate their recognition sites but pairs of sites in inverted repeat will always remain protected following semi-conservative replication (2,8–10).

To account for how ATP hydrolysis allows long-range communication between sites in an oriented manner, a number of models have been suggested based on unidirectional 1D DNA translocation accompanied in part by accessory DNA loops (3,11–13). These models are principally based on similarity to the domain organization of the Type I REs, for which motor driven unidirectional DNA translocation has been unambiguously shown [(14) and references therein, (15–17)]. However, Type III REs utilize at least 1000-fold less ATP than their Type I counterparts (3,10,18,19), which has significantly challenged the 1D translocation hypothesis. To resolve this contradiction, additional 3D DNA looping steps preceding 1D translocation have also been suggested to shorten the necessary translocation distance (12).

Using single-molecule and bulk solution DNA cleavage assays we recently provided evidence that the communication occurs in 1D along the DNA contour (5,19). Additionally the communication was found to be bidirectional, since the cleavage efficiency on linear DNA was significantly increased if a bulky protein roadblock was incorporated at the DNA ends. Based on these observations, we proposed an alternative scheme in which ATP hydrolysis by an enzyme at a target site initiates a diffusive bidirectional motion on DNA (Figure 1) (1,19). In this model diffusion does not require ATP hydrolysis and maintains the orientation of the enzyme on the DNA as set by the direction of the target site. Cleavage occurs once a sliding enzyme collides 'head-on' (i.e. in a HtH manner), with a second enzyme that is bound to its target site.

*To whom correspondence should be addressed. Tel: +49 351 463 40333; Fax: +49 351 463 40342; Email: ralf.seidel@biotec.tu-dresden.de
Correspondence may also be addressed to Mark D. Szczelkun. Tel: +44 117 928 7439; Fax: +44 117 928 8274; Email: mark.szczelkun@bristol.ac.uk

The authors wish it to be known that, in their opinion, the first two authors should be regarded as joint First Authors.

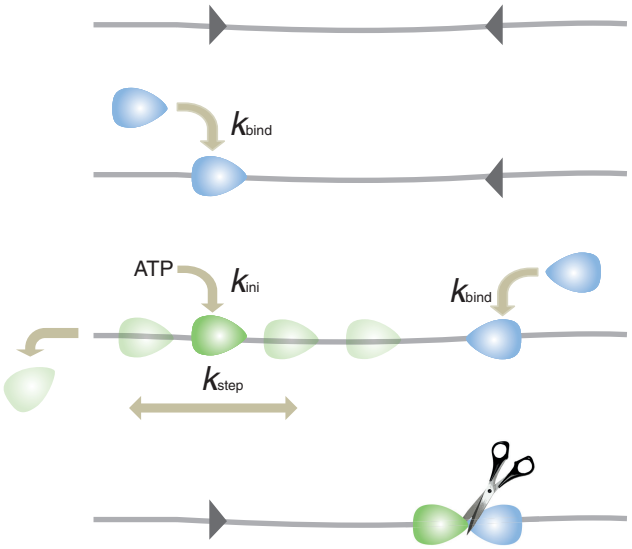

Figure 1. Sliding model for long-range communication on DNA by Type III restriction enzymes. Type III restriction enzymes (blue ellipsoids) bind to their recognition sites (dark gray triangles) with rate k_{bind}. Site specific DNA binding induces hydrolysis of ATP and the enzyme switches stochastically to a sliding mode with a rate k_{ini} and undergoes 1D diffusion along the DNA contour (shown by colour change to green). Sliding occurs in a random walk-like fashion in both directions with equal probability, independent of ATP hydrolysis, at a stepping rate k_{step}. When a sliding enzyme collides in a 'head-on' orientation with a second enzyme that is statically bound to its site, cleavage of DNA is triggered. The DNA shown is a two-site substrate with sites in head-to-head orientation. Animated examples of one round of the model based on MC modelling are shown for a head-to-head and also a tail-to-tail substrate in Movies S1 and S2 respectively in Supplementary Data.

This 'DNA sliding' model can account for the low ATP consumption during cleavage, the site orientation selectivity, the force-independence of cleavage and the inhibitory effect of open DNA ends (see below). Nonetheless, the actual communication model for Type III REs is still being debated (20).

An important experimental observation is that, under standard reaction conditions, cleavage of a two-site DNA substrate by a Type III RE produces a double-strand break downstream of just one of the two sites. No further cleavage occurs on that DNA molecule (4,10,21). Although one of the sites remains intact, this cleavage activity would be perfectly sufficient for the *in vivo* role of Type III enzymes in preventing phage infection since just one dsDNA break would be lethal to the parasitic nucleic acid. To further challenge the 1D diffusion hypothesis, we sought to answer the following question: what selective pressures determine which of the two sites is cut? By using alternative DNA substrates and by varying the concentration of enzyme, we introduced asymmetry into the communication process that changed the cleavage pattern in a reproducible and testable manner. The empirical data was directly compared to Monte–Carlo (MC) simulations based on the sliding-cleavage scheme (Figure 1). The close correspondence of the two data sets provides further evidence for bidirectional motion on DNA with cleavage occurring upon head-on collision between a sliding and a static enzyme.

MATERIALS AND METHODS

Proteins

EcoPI and EcoP15I were purified as described previously (6). Protein concentrations were determined from the absorption at 280 nm using extinction coefficients derived from the aromatic amino acid composition in the predicted amino acid sequences. Concentrations are reported in terms of a Res_2Mod_2 heterotetramer. All other enzymes were obtained from New England Biolabs (MA, USA) and used as recommended by the manufacturer.

DNA

Synthetic oligonucleotides were purchased from Eurofins-MWG Operon (Ebersberg, Germany). pKA9 (−R1, +N) was generated as follows. pMDS33 (4), was partially digested by SfiI, ligated with annealed oligonucleotides 5′-ACCTCAGCATGCGGCCGCTAACTA GTCATCTAGATAGGTACCAAC-3′ and 5′-GGTACC TATCTAGATGACTAGTTAGCGGCCGCATGCTGA GGTGTT-3′, and clones selected for insertion at the SfiI site located at 1611 bp to generate pMDS33 (MCS). An EcoPI site in the kanamycin resistance cassette of pUC4K (22), was mutated by QuikChange Mutagenesis (Agilent Technologies, CA, USA) using the primers 5′-CGAGTCG GAATCGCTGACCGATACCAGGAT-3′ and 5′-ATCC TGGTATCGGTCAGCGATTCCGACTCG-3′, and the cassette amplified by PCR using primers 5′-GAGGTAC CGCGTGATCTGATCCTTCAAC-3′ and 5′-ATAGGT ACCGAGTCAGTGAGCGAGGAAGC-3′. The PCR product and pMDS33 (MCS) were cleaved with KpnI and ligated to generate pAMS1. The three EcoP15I sites in pAMS1 were removed by three consecutive rounds of QuikChange Mutagenesis using primer pairs 5′-CGCCAC TGGCAGCCGCCACTGGTAAC-3′ and 5′-GTTACCA GTGGCGGCTGCCAGTGGCG-3′, 5′-GTTTGCAAGC AGCCGATTACGCGCAG-3′ and 5′-CTGCGCGTAAT CGGCTGCTTGCAAAC-3′, 5′-CTCTGCTCAAGCC AGTTACC-3′ and 5′-GAGACGAGTTCGGTCAAT GG-3′. The resulting plasmid, pAMS10, was cut with SfiI and ligated with annealed oligonucleotides 5′-ACTA GAAGGACAGTATTTGGTATCTGCGCTCTGCTGA AGCCAGTT-3′ and 5′-TGGCTTCAGCAGAGCG CAGATACCAAATACTGTCCTTCTAGTAAC-3′. The kanamycin resistance gene in the resulting plasmid, pKA4, was found to cause problems during DNA preparation (data not shown). Therefore, pKA4 was digested with KpnI, the DNA re-ligated and recombinants selected for loss of the kanamycin resistance gene to generate pKA9. A 727-bp region of pKA9 containing a single Tn*21* resolvase res site was then removed by digestion with NdeI and BsaAI, the DNA re-ligated and clones selected by the absence of cleavage with NdeI. Finally, an NdeI site was reintroduced by PCR using the primers 5′-ATGTCGCGCGTTTCGGTGATGAC-3′ and 5′-ATG

ACGAAAGGGCCTCGTGATAC-3′ to produce pKA9 (−R1, +N).

To prepare DNA for biochemical assays, *Escherichia coli* Top10 (Invitrogen, CA, USA) or XL10-Gold (Agilent Technologies) were transformed with the required plasmid, grown in LB medium and the DNA extracted using either commercial protocols (Qiagen, Hilden, Germany) or by density gradient centrifugation in CsCl-ethidium bromide (23). We have not noted any difference in Type III activity between the different preparation methods. For experiments requiring ^{3}H-labelled DNA, transformants were grown in M9 minimal medium supplemented with 37 MBq/L [^{3}H-methyl] thymidine (PerkinElmer, MA, USA).

Linear DNA substrates were generated by PCR amplification or by digestion by Type II restriction enzymes. For substrates with two pairs of EcoPI and EcoP15I sites (Table 1, Figures 2 and 3), regions of either pJT1.1 (HtH) or pJT1.3 (TtT) (5) were amplified using Pfu polymerase (Promega) or Phusion polymerase (Finnzymes, New England Biolabs), following the manufacturer's standard protocols. To generate DNA with biotin labels at either both ends ('blocked end') or at just one end ('open end'), the PCR reactions contained the 5′-biotinylated primer 5′-Biotin-CAGTGTTATCACTCA TGGTTATGGCAGCA-3′ and either 5′-biotinylated or unmodified versions of 5′-CTTTATGCTTCCGGCTCG TATGTTG-3′ for the ∼100-bp spacings, 5′-ATGCAGC TGGCACGACAGGTTTC-3′ for the ∼200-bp spacings, 5′-GGGTTTCGCCACCTCTGACTTG-3′ for the ∼500-bp spacings and 5′-CGCGTAATCTGGTGCTTG CAAACAAAAAAAC-3′ for the ∼1000-bp spacings (Figure 2A and Table 1). The DNA was then purified using a PCR purification kit (Qiagen) and eluted in H_2O. For mixed substrates with a pair of EcoPI and EcoP15I sites in HtH repeat (Table 1 and Figure 4), pKA9 (−R1, +N) was digested with NdeI and the linear DNA purified by phenol/chloroform extraction followed by ethanol precipitation. End-labelling of the DNA with biotin was carried out using Klenow (3′–5′ exo-) polymerase and biotin-dUTP (5). The labelled DNA was further purified by phenol/chloroform extraction followed by ethanol precipitation.

DNA concentrations were determined from absorbance at 260 nm, assuming an extinction coefficient of $0.02\,ml\,\mu g^{-1}\,cm^{-1}$ and a DNA molecular weight of 6.6×10^{5} Da kbp^{-1}.

Table 1. Distances for the DNA substrates

Enzyme(s)	Site orientation	DNA #	dsDNA distances (bp)		
			a	*b*	*c*
EcoPI	HtH	1	105	114	1007
		2	204		
		3	503		
		4	1004		
	TtT	5	120	84	1024
		6	219		
		7	518		
		8	1019		
EcoP15I	HtH	1	101	120	1003
		2	200		
		3	499		
		4	1000		
	TtT	5	123	76	1027
		6	222		
		7	521		
		8	1022		
EcoPI and EcoP15I	HtH	9	1205	1915	522

Distances are defined as follows (Figures 2–4): *a* is the distance from the leftward dsDNA end to the base pair 5′ to Site 1; *b* is the distance from the base pair 3′ to Site 1 to the base pair 5′ to Site 2; and, *c* is the distance from the base pair 3′ to Site 2 to the rightward dsDNA end. To minimize DNA handling, DNA #1 to #8 had a pair of HtH or TtT sites for both EcoPI and EcoP15I; one DNA could therefore be used as a substrate for either EcoPI or EcoP15I.

Cleavage reactions

DNA substrates (2 or 10 nM, as indicated) were preincubated for at least 1 min at 25°C in Buffer R^{+} [50 mM Tris–HCl, pH 8.0, 50 mM KCl, 10 mM $MgCl_2$, 1 mM DTT, 0.01% (w/v) BSA] supplemented with 4 mM ATP and streptavidin at a 50-fold molar excess over DNA. Reactions were initiated by adding the enzyme(s) at the concentration(s) indicated, incubated at 25°C for either 5 min (EcoP15I on HtH DNA), 10 min (EcoPI and EcoP15I on the mixed DNA) or 15 min (all other reactions). We verified that the reactions were run to completion in each case (data not shown). Reactions were subsequently quenched by addition of 1/2 volume of STEB buffer [0.1 M Tris–HCl, pH 7.5, 0.2 M EDTA, 40% (w/v) sucrose, 0.4 mg/ml bromophenol blue]. Then 0.1 volume of biotin [0.2 mg/ml in 50 mM Tris–HCl (pH 8.0)] was added to each aliquot and the samples heated for at least 5 min at 80°C to prevent anomalous electrophoretic mobility due to bound streptavidin and restriction enzymes. The DNA substrates and products were separated by agarose gel electrophoresis. Due to the low DNA concentrations used, some small DNA fragments were not detected. To calculate cleavage site distributions, the DNA bands for the longest cleavage product at either site (Figures 2B, 4B and Supplementary Figure S1) were quantified either from digital images of ethidium bromide-stained gels captured on a UVP GelDoc-It Imaging System using a linear intensity scale or by scintillation counting (23). In each case quantified values were corrected for differences in DNA size assuming a linear relationship between dsDNA length and signal.

We estimated the error of the measured cleavage site distribution from all measurements made on symmetric substrates (i.e. with both ends being closed and with $a = \sim 1000$ bp), which should nominally be cleaved with a 50:50 distribution (Figure 3). From 13 individual experiments (two different enzymes, two different site orientations and three to four repeats for each condition) we obtained a mean of 48.7% and a standard deviation of 4.0% for cleavage at Site 1—the latter value equating the standard error of an individual measurement. In order to exclude accidental errors and potential bias from a particular DNA or enzyme preparation, all cleavage experiments were repeated between two to four times. The repetitions always reproduced the initial measurements

within small errors (see standard deviations in Supplementary Figure S2).

MC simulations

MC simulations as described in the main text were programmed in LabVIEW (National Instruments Inc.) and run on a workstation with a dual quad core 2.66 GHz processor (Dell, T5400-Intel Xeon E5430). The statistical error of the simulations for the normalized cleavage probability p_X at a given site X ($X = 1, 2$) was calculated as twice the standard error (95% confidence interval) of a binomial distribution normalized by the total number of simulations N_{tot} that ended in cleavage: $\mathrm{Err}(p_x) = 2\sqrt{p_x(1-p_x)/N_{tot}}$ with $p_X = N_X/N_{tot}$ and N_X being the number of cleavage events at site X.

RESULTS AND DISCUSSION

Experimental rationale

Our previous analysis of the Type III REs has concentrated on the related proteins EcoPI (which recognizes 5′-AGACC-3′) and EcoP15I (which recognizes 5′-CAGCAG-3′). To test the sliding model we investigated DNA cleavage rates as an indirect measure of the site-to-site communication rate. By changing the length of the DNA between a pair of identical sites or by varying symmetrically the distance between the sites and the DNA ends we sought to observe changes in the cleavage rate that could be related to possible communication models (5,19). Because the sites were identical in these cases, site selection was 50:50 regardless of orientation [as in (4)]. However, we were unable to observe any systematic change in the cleavage rate that could be fitted to either 1D diffusion or translocation models. An explanation for this may be that the communication process is significantly faster than the binding or cleavage steps and is thus kinetically masked.

As an alternative approach to test the validity of the sliding model and its mechanistic assumptions we addressed here how this mode of communication affects the relative cleavage site distribution on *asymmetric* two-site linear DNA substrates. To introduce sufficient asymmetry into the reaction pathway we applied two different strategies.

Introducing bias due to end-blocking and end-spacing effects. The sliding model indicates that on linear DNA a Type III RE cannot exit at a DNA end that is 'blocked' (e.g. by biotin–streptavidin) but it can exit from an 'open' end (1,19). Consequently, RE activity is efficient when both ends are blocked but inefficient when both ends are open. This difference could be exploited by using linear DNA molecules in which one DNA end differed from the other end in terms of distance to a site and by being either blocked (by biotin–streptavidin) or open. A single open end will asymmetrically deplete the sliding enzyme population producing characteristic changes in the cleavage site distribution (discussed below).

Introducing bias due to increased initiation at one site. As a comparative approach, the cleavage at one site over another could be biased by increasing the total amount of sliding enzyme that originated from only one of the two sites. For this a mixed HtH linear DNA substrate could be used with one recognition site for EcoPI and one recognition site for EcoP15I (Table 1 and Figure 4A). EcoPI and EcoP15I are very similar enzymes (amino acid identity >90% in the Res subunit and >60% in the Mod subunit) and can cooperate to cleave a mixed DNA substrate (24,25). By varying the concentration of one enzyme over the other, the corresponding increase in communicating species originating from one site will also influence the relative cleavage distributions in a characteristic manner (discussed below).

Distribution of cleavage on head-to-head substrates with end bias

To apply the first strategy described above, we generated a family of linear HtH and TtT DNA substrates with biotin–streptavidin blocks at either one end ('open end' substrates) or both ends ('blocked end' substrates). We first tested the HtH DNA illustrated in Figure 2A. As drawn, we arbitrarily define the site closest to the left end as 'Site 1' and the other site as 'Site 2'. The distance a from Site 1 to its neighbouring open or blocked end was varied whilst the inter-site distance b of ~100 bp and the distance c from Site 2 to its neighbouring blocked end of ~1000 bp were kept constant (see 'Materials and Methods' section and Table 1). To avoid any differences resulting from a preference for cleavage at particular sequences flanking the target site, we used pairs of Type III sites with identical sequences up- and down-stream of the sites. Thus, any observed asymmetry in the cleavage preference would be due to variation in distance a and/or to the difference in end capping.

Based on an intuitive consideration of the sliding model (Figure 1), an 'open end' HtH substrate would asymmetrically deplete the sliding enzyme population as follows. Enzymes that initiate sliding from Site 1 would be more likely to dissociate from the neighbouring open end than enzymes that initiate sliding from Site 2. This would reduce the chance of enzymes initiating from Site 1 reaching Site 2. Correspondingly, cleavage would occur more often at Site 1. If distance a were then shortened, we would expect this bias in cleavage at Site 1 to increase. In contrast, on the 'blocked end' HtH substrates, enzymes initiating from either Site 1 or Site 2 will have an equal chance of dissociation and the cleavage will distribute 50:50, regardless of any change in distance a. The bias in cleavage site distribution on the open end substrates would not be observed assuming the alternative communication models based on unidirectional motion, which instead would give 50:50 distributions on all DNA tested regardless of end-capping.

The HtH DNA substrates were incubated with either EcoPI or EcoP15I for a fixed time, the reactions stopped, the substrates and products separated by agarose gel electrophoresis, and the DNA quantified by ethidium bromide staining and gel densitometry see

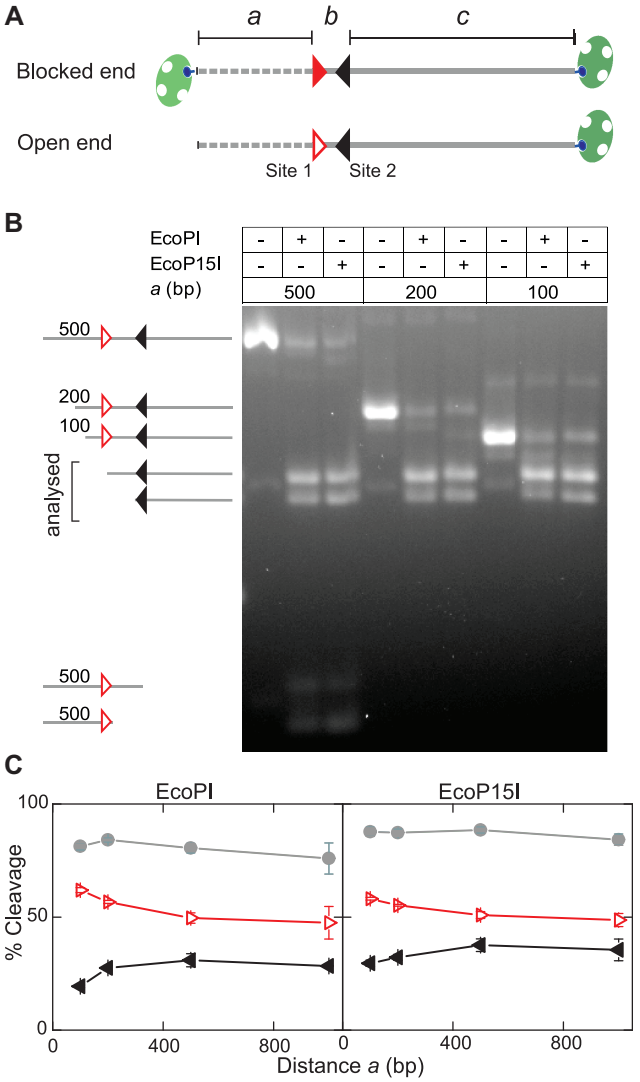

Figure 2. Using end-spacing effects to introduce bias into the distribution of cleavage between two sites. (**A**) DNA substrates (see 'Materials and Methods' section). Triangles denote the orientation of the EcoPI (5′-AGACC-3′) or EcoP15I (5′-CAGCAG-3′) recognition sites. Sites 1 and 2 are defined as the sites being closest to the leftward or rightward end, respectively. The Site 1 triangles are either 'solid' (to denote a blocked end) or 'open' (to denote an open end). Green ovals represent streptavidin molecules attached to biotin-labelled DNA ends (blue circles). Distances *a*, *b* and *c* for each substrate are listed in Table 1. Distance *a* was varied as indicated by the dashed line. Each DNA had a pair of sites for both EcoPI and for EcoP15I (only one pair of sites for one enzyme is shown for clarity) (Table 1). (**B**) Example agarose gel for the open end HtH substrates with distance $a = \sim 100$, ~ 200 and ~ 500 bp. See Supplementary Figure S1 for the same gel including a DNA size marker and the lanes for $a = \sim 1000$ bp. Reactions contained 10 nM DNA and 75 nM EcoPI or EcoP15I and were incubated for 15 min with EcoPI or 5 min with EcoP15I. DNA samples were separated by agarose gel electrophoresis. Resulting cleavage products are illustrated by cartoons. Except for $a = \sim 500$ bp, the two smaller cleavage products that include the short end *a* were not visible on the gel. Cleavage at Site 1 was quantified from the DNA product containing domains *b* and *c;* cleavage at Site 2 was quantified from the DNA product containing domain *c* alone (see 'Materials and Methods' section). (**C**) Percentages of Site 1 cleavage (red open triangles), of Site 2 cleavage (solid black triangles) and total cleavage (solid grey circles) for the gel shown in B as function of distances *a*. Points and error bars are the average and standard deviation from two to four repeat experiments. See Supplementary Figure S2 for all data, including the standard deviations, which illustrate the high reproducibility of the measurements.

'Materials and Methods' section). An example gel using the open end DNA is shown in Figure 2B and Supplementary Figure S1. The corresponding quantified data averaged from multiple repeat experiments is shown in Figure 2C (quantified data from experiments with all DNA substrates are presented in Supplementary Figure S2). Total DNA cleavage does not reach 100% under these reaction conditions, most likely due to competing DNA methylation (4).

For the blocked end HtH substrates, cleavage was distributed equally between each site with no dependence upon distance *a* (see Figure 3A, left panel, for data normalized by the total amount of cleaved DNA). In contrast, on the open end HtH DNA both EcoPI and EcoP15I demonstrated differences in the relative cleavage between the sites that varied as a function of distance *a* (Figure 3A, right panel): in both cases a preference for cleavage at Site 1 was observed and this preference became more pronounced as distance *a* was shortened. These observations are consistent with the predictions described above based on the sliding model.

MC simulations of cleavage site selection

To provide more objective predictions of these effects that can then be compared to the empirical data, we employed MC simulations based on the simplest possible realization of the sliding model. Each DNA substrate was modelled as a linear lattice of non-specific protein binding sites 1-bp apart and including two specific interaction sites at locations corresponding to the enzyme target sites for the DNA being considered. The dynamics of protein–DNA interaction were described by just three rates (Figure 1): k_{bind}, the binding rate of an enzyme to a specific site; k_{ini}, the rate at which a specifically bound enzyme switches into the sliding state; and k_{step}, the rate at which an enzyme in the sliding state makes a single 1-bp random walk step either leftward or rightward on the lattice (with equal probability). At each step of the simulation cycle, we calculated whether enzymes had bound, initiated or stepped along the DNA. Where an enzyme reached an end of the lattice which was open, a step off the lattice caused dissociation. Where an enzyme reached an end of the lattice which was blocked, dissociation did not occur. When a sliding enzyme collided with an enzyme bound at a recognition position in a head-on orientation, cleavage at that site was scored and another round of simulation undertaken (see Movie S1 in Supplementary Data for an example simulation). The model stochastically allowed for the accumulation of multiple enzymes on the DNA, taking into account the molar excess of enzyme used in the experiments. Additional dissociation from internal sites during sliding was not considered in the data presented in order to keep the model as simple as possible. However, when included it did not alter the outcome of the simulations (data not shown). Rate constants used in our simulations (see below) are given as probabilities per 1-bp random walk step and cannot be considered as absolute values but instead as relative values, since only the reaction end-point is measured. According to its definition, k_{step} equals a nominal value

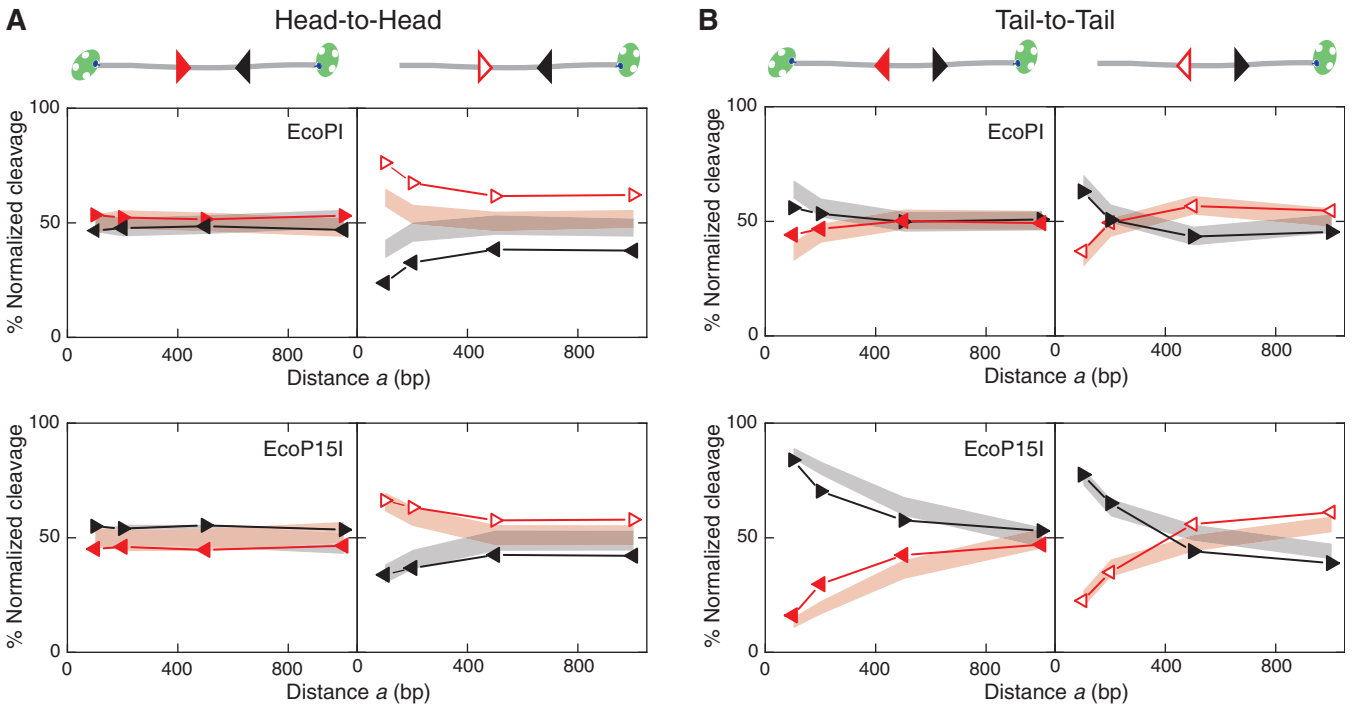

Figure 3. Normalized cleavage site distribution compared to MC simulations. (**A**) HtH constructs and (**B**) TtT constructs, with blocked or open ends. The experimentally-determined percentages of Site 1 cleavage (solid or open red triangles) and of Site 2 cleavage (solid black triangles) were normalized by the total fraction of cleaved DNA. Percentages of cleavage determined from MC simulations are shown as light red (Site 1) and grey (Site 2) areas, which cover the 95% confidence intervals around the mean percentage for at least 500 simulations. Rates used in the simulations, given as probability per 1 bp random walk step, are indicated in the main text.

of 1. For the initial modelling of the HtH and TtT substrates, k_{bind} and k_{ini} were adapted to fit the experimental data. For subsequent simulations we modelled 5 bp instead of 1bp random walk steps in order to save computation time. This provided identical results compared to the 1-bp steps (data not shown) but required on average 25-fold less simulation steps. For each condition (DNA end length, end capping), at least 500 cleavage events were simulated to obtain acceptable statistical accuracy.

Both MC model data and empirical data showed good qualitative agreement, independent of the particular value of k_{ini} (Figure 3A). Best overall agreement (also including TtT and mixed substrates, see below) was obtained by choosing $k_{bind} = 4 \times 10^{-8}$ for both enzymes, and $k_{ini} = 4 \times 10^{-6}$ for EcoPI and $k_{ini} = 4 \times 10^{-8}$ for EcoP15I. Note that other sets of k_{bind} and k_{ini} can also describe the experimental data in Figure 3 as long as the ratio between the rates is preserved (Supplementary Figure S3). Considering published diffusion constants for enzymes sliding along DNA in the order of $10^6\,bp^2\,s^{-1}$ (26,27), the chosen value for $k_{bind} = 4 \times 10^{-8}$ in these simulations would correspond to a 'real' enzyme binding rate in the order of $\sim 0.1\,s^{-1}$. A faster initiation rate for EcoPI, and thus shorter-lived binding state, compared to EcoP15I was also suggested previously to explain the difference between the enzymes in relative cleavage rates of TtT substrates compared to HtH substrates (5). The agreement between both the simulated and empirical data sets in Figure 3A validates our predictions and provides evidence that the sliding model can account for the relative cleavage of a site in a HtH oriented substrate dependent on its proximity to a DNA end.

Distribution of cleavage on tail-to-tail substrates

In addition to sites in HtH arrangements we also tested similar substrates with the sites in TtT arrangement (Figure 3B, Table 1, and Supplementary Figure S2). On these substrates, cleavage that would be triggered by head-on collision requires that the sliding enzyme actually bypasses a site before the second enzyme binds (1,5). Consequently, the efficiency of cleavage of TtT DNA can be affected by the binding lifetime at the site: the more often the site is occupied, the less chance that a sliding enzyme can bypass the site.

The reactions were carried out and analysed as above. Quantified and normalized data from repeat experiments using either EcoPI or EcoP15I are shown in Figure 3B. In contrast to the data on HtH DNA, we observed quite different outcomes on the TtT DNA that depended on both the enzyme used and the characteristics of the DNA substrate:

EcoPI on blocked end TtT DNA. Where distance *a* was 518 or 1019 bp, the cleavage distribution between Sites 1 and 2 was equal, within experimental variation. However, at the shorter *a* distances (120 or 219 bp), cleavage at Site 2 increased moderately.

EcoPI on open end TtT DNA. Where distance *a* was 518 or 1019 bp, a small but significant preference was observed for cleavage at Site 1. However, as *a* was shortened, the relative preference switched until Site 2 was preferred at $a = 120$ bp.

EcoP15I on blocked end TtT DNA. Where $a = 1022$ bp, the cleavage distribution between Sites 1 and 2 was equal, within experimental variation. However, as *a* was shortened, cleavage at Site 2 increased significantly. When $a = 123$ bp, cleavage at Site 2 accounted for >80% of the total cleavage. A reduction in the total cleavage efficiency was also observed as *a* was reduced (Supplementary Figure S2).

EcoP15I on open end TtT DNA. As for EcoPI above, Site 1 was preferred at longer distances of *a,* whilst Site 2 was preferred at shorter distances of *a*. However, the contrast was more marked. There was also a more marked reduction in overall cleavage as *a* reduced which was not observed to the same extent with EcoPI (Supplementary Figure S2). Strikingly, the overall pattern in this data looks similar to that observed using EcoP15I and the blocked end TtT DNA.

The feature common to all the TtT data is that cleavage of Site 2 is preferred to Site 1 at short distances of *a*, the opposite of what was observed with HtH DNA. Moreover, this preference was still observed when both ends were blocked, again the opposite of what was observed with HtH DNA.

We tested whether the observed profiles could still be explained within the framework of the sliding model by simulating the cleavage of TtT DNA using the MC simulations, as above (Movie S2 in Supplementary Data). Both simulated and empirical data show very clear agreement using the same rates chosen for the HtH simulations (Figure 3B). This demonstrates that the measured cleavage site selection is exactly what one would expect from a bidirectional sliding model with head-on collision causing cleavage at a site.

The increase in cleavage at Site 2 relative to Site 1 at small distances may seem counterintuitive, particularly when compared to the data obtained using HtH site arrangements. However, our observations can also be rationalized using the sliding model: On both HtH and TtT DNA, the population of enzymes that initiates sliding from Site 1 will be reduced if there is a proximal open end. Therefore, less of these enzymes reach Site 2 and cleavage at Site 1 increases. However, for TtT DNA, cleavage at Site 1 additionally requires that the sliding enzyme coming from Site 2 enters the DNA domain between the DNA end and Site 1 (i.e. defined as domain *a*, Figure 2A) and subsequently becomes trapped there by a second enzyme binding to Site 1. As domain *a* shortens, the chance of this trapping event reduces. Thus, less of the sliding enzymes that started at Site 2 reach Site 1 in a head-on orientation and relative cleavage at Site 2 increases. It appears that the reduced 'trapping efficiency' that is specific to TtT DNA is the dominant effect for short distances of *a* while the depletion of enzymes that start near an open end becomes more dominant for longer distances of *a*. The clear switch in preference on the open end substrates can therefore be explained.

An additional limitation for TtT DNA is that binding of an enzyme to Site 1 blocks sliding enzymes from entering domain *a*. For EcoP15I this effect is more dominant than the trapping effect above since TtT DNA is cleaved less efficiently than HtH DNA (5). A tight binding of EcoP15I most likely causes the reduction in overall cleavage efficiency seen here as domain *a* shortens (Supplementary Figure S2).

Overall, the observation of differences between HtH and TtT DNA are consistent with a sliding model where the cleavage state requires a head-on protein-protein contact.

Distribution of cleavage as a function of enzyme loading

As an alternative way to bias cleavage at one location over another, we generated a mixed DNA substrate with recognition sites for EcoPI and EcoP15I in HtH orientation (Figure 4A and Table 1). The substrate was capped at both ends with streptavidin to ensure efficient cleavage and to prevent bias due to end effects (i.e. as in Figure 3). DNA cleavage only occurs when both enzymes are added (data not shown). By varying, for example, the concentration of EcoPI whilst keeping EcoP15I constant, the sliding model predicts that the population of EcoPI molecules sliding on DNA will increase relative to EcoP15I. In turn this would result in a concentration-dependent increase in cleavage at the EcoP15I site relative to the EcoPI site.

To test this prediction the mixed DNA substrate was incubated with a fixed concentration of EcoP15I and with a varying concentration of EcoPI for a fixed time, the reactions stopped, the substrates and products separated by agarose gel electrophoresis, and the DNA quantified by scintillation counting (see 'Materials and Methods' section). An example gel is shown in Figure 4B, whilst the average quantified data is shown in Figure 4C, left panel. With an equal concentration of EcoPI and EcoP15I, a small but significant preference for cleavage at the EcoPI site was observed. As the concentration of EcoPI was increased relative to EcoP15I, the total cleavage reduced from ~96% to ~82%, reflecting either an increase in inhibition by co-methylation or a general decrease in activity due to non-specific inhibition by the excess EcoPI. In addition, the distribution of cleavage loci changed—cleavage at the EcoPI site decreased to a minimum of ~25% while the total cleavage at the EcoP15I site increased to a maximum of ~75% (as percentages of the total cleavage). Overall this pattern matches what one would expect based on a simple consideration of the sliding model.

The data was normalized by the total cleavage and compared to MC simulations using the same k_{bind} and k_{ini} values as used above, i.e. $k_{bind} = 4 \times 10^{-8}$ for both enzymes, and $k_{ini} = 4 \times 10^{-6}$ for EcoPI and $k_{ini} = 4 \times 10^{-8}$ for EcoP15I (Figure 4C, right panel). The empirical and simulated data show very good correspondence, providing further evidence of the validity of the simple sliding scheme in Figure 1. Note that in contrast to the single

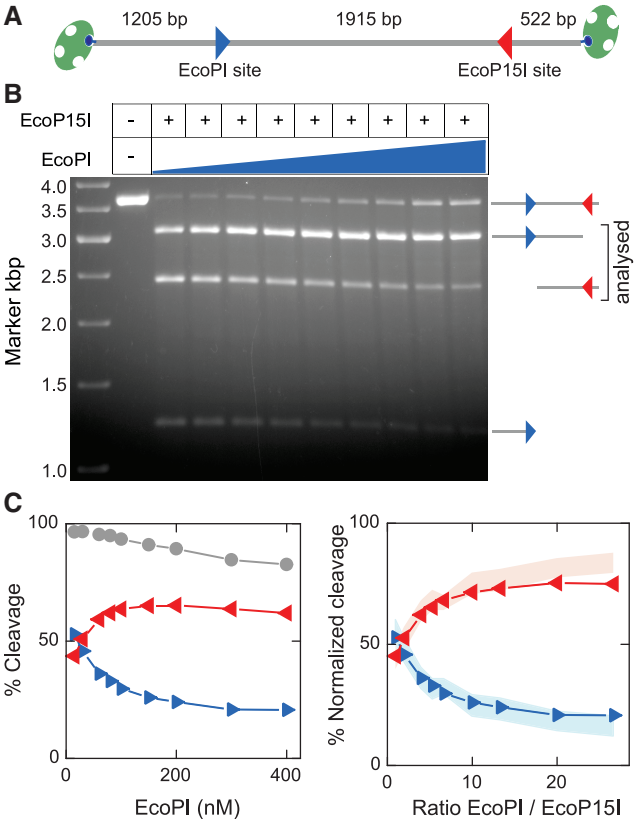

Figure 4. Using increased initiation from one site to introduce bias into the distribution of cleavage between two sites. (**A**) Scheme of the mixed DNA substrate comprising one EcoPI recognition site (solid blue triangle) and one EcoP15I recognition site (solid red triangle) in a HtH orientation. (**B**) Example agarose gel for cleavage experiments using the mixed substrate. Reactions contained 2 nM DNA, 15 nM EcoP15I and 15–400 nM EcoPI and were incubated for 10 min. Resulting cleavage products are illustrated by sketches. The short ~540 bp fragment from cleavage at the EcoP15I site was not visible on the gel. Cleavage at the EcoPI and EcoP15I sites was quantified from the bands indicated. (**C**) Comparison of empirical and simulated DNA cleavage patterns as a function of EcoPI concentration. (Left panel) Percentages of EcoPI site cleavage (blue triangles), of EcoP15I site cleavage (red triangles) and total cleavage (grey circles). Points are the average from three repeat experiments. Calculated standard deviations are smaller than the symbol size illustrating the high reproducibility of the measurements. (Right panel) Normalized percentages of cleavage at the EcoPI and EcoP15I sites compared to the MC simulation data, shown as light blue (EcoPI site) and light red (EcoP15I site) areas, which cover the 95% confidence intervals around the mean percentage for at least 500 simulations. Rates are the same as those in Figure 3 (see main text).

enzyme substrates, faster values for k_{bind} and k_{ini} fail to describe the data obtained with the mixed substrates (Supplementary Figure S3).

CONCLUSION

It is well known that non-specific DNA sequences adjacent to a RE target site can affect protein binding due to indirect interactions. Additionally for the Type III REs, cleavage is targeted to the non-specific DNA 25–28 bp downstream of the site. Therefore the nuclease domain may show a catalytic preference for certain sequences. Using EcoP15I plasmid substrates, a systematic study showed that variations in sequence around the CAGCAG sequence at one site can cause alterations in the relative cleavage pattern independent of DNA ends (21). Whilst this data indicates that Type III REs can have a preference for cleaving certain sequences, it does not address the underlying mechanism of communication. In the experiments presented here we instead observed long-range effects on the cleavage preference at a pair of identical sites due to variations in site location (in particular the distance to a DNA end and whether it was blocked or free) or due to variations in the concentration of a Type III enzyme initiating from one of the two sites. In addition, these variations in preference were dependent on whether the sites were in HtH or TtT orientation. In each case the data could be explained using a simple DNA sliding model, backed-up by MC simulations, that is based on a 1D bidirectional motion of the enzymes on DNA and cleavage that is activated upon head-on collision between one sliding enzyme and one static enzyme (Figure 1, Movies S1 and S2 in Supplementary Data).

In combination with previous bulk solution and single molecule results, the empirical and simulated data presented here provide strong evidence in favour of the proposed sliding mode for long-range communication of Type III enzymes. However, there is still a considerable debate in the field as to whether or not DNA loops play any role in the communication scheme (1,20). A series of AFM studies argued for extensive looping being induced by passive 3D diffusive loop capture and by active 1D translocation driven loop expansion (12,13). In contrast single-molecule magnetic tweezers assays at fN forces that hardly perturb the random coil configuration of the DNA did not obtain evidence for loops that persisted longer than 1 s (19).

So far the discussion about whether 'to loop or not to loop' has not been very clear in distinguishing whether looping itself is responsible for the inter-site communication or whether looping just plays an accessory role. The data we present here cannot provide evidence to refute the existence of short-lived loop states. However, it would be very difficult to explain the different cleavage preferences we observed in terms of any bias due to communication by 3D looping. It is a long-held view in the field of DNA–protein transactions that passive 3D DNA looping cannot provide: (i) site orientation selectivity, except under special circumstances of DNA topology or short intersite spacings and (ii) a bias for interactions between sites on the same DNA as opposed to separate but topologically linked DNA.

The first point is illustrated by a study of the Type II RE BspMI, where site orientation selectivity was observed as a function of intersite spacing and DNA topology (28). A bias for the geometry of a DNA loop [preferentially trapping a negative or positive node (29)] was only obtained for very short intersite spacings (<170 bp). The Type III REs still show orientation selectivity over many thousands of bp. A bias for the interaction geometry over such long distances is well established for many

site-specific recombinases, which however requires an absolute dependence on negatively supercoiled DNA (30–32). In contrast, cleavage rates for Type III REs on linear and negatively supercoiled DNA are more or less identical (4,19). Inhibition on positively supercoiled DNA (25), most likely reflected the extreme levels of DNA twist introduced into those DNA preparations (33).

The second point is illustrated by a wide range of studies of 3D DNA looping by REs using concatenated DNA [e.g. (34–38)], where cleavage could occur when sites were both on the same DNA and also on separate but topologically interlinked DNA rings. This simply reflects the fact that the local site concentration can be elevated by either 1D or 3D connectivity. Again, and in contrast to all these examples, the Type III REs could not cut sites on separate rings of a catenane (6), arguing against 3D looping as a critical step in selecting directionality.

Within any communication model however, DNA looping could play an accessory role rather than being a stringent requirement. This is consistent with the fact that inhibition of looping by DNA stretching has no significant influence on the communication and cleavage kinetics of Type III REs (19), in agreement with data using restriction enzymes that interact only with a single site (39), but in stark contrast to restriction enzymes that obligatorily use 3D looping (40,41). Also the sliding model, and thus the data presented here, is still compatible with the formation of transient loops during bidirectional 1D motion that are shorter lived than ~1 s (19). This may in fact be an attractive option to resolve the controversy between AFM measurements and single-molecule magnetic tweezers measurements (20). However, we also note that there are still severe discrepancies between the two data sets, since in the AFM experiments the equilibrium is shifted towards a compacted and heavily looped configuration, while for the tweezers experiments the equilibrium configuration is predominantly non-looped, and only allows for rare transient looping. Thus, further work is still required to resolve the contribution of DNA-looped states in inter-site communication by Type III restriction enzymes.

We suggest that the positional effects observed here (Figures 2 and 3), might also be observed in other processes, such as DNA mismatch repair, where communication by DNA sliding has also been suggested to occur (1). Similar experiments could therefore provide corroboratory evidence for other diffusing enzyme systems. In addition, and beyond the academic interest in understanding the cleavage site selection, our observations may be useful for biotechnological reasons. Since these enzymes cut at 'long' distances from their target sites they are used in mate-pair library preparations for next generation sequencing to study chromosome structural rearrangements (42). Our observations could be exploited to help increase the efficiency of library preparations by the Type III REs.

SUPPLEMENTARY DATA

Supplementary Data are available at NAR Online.

ACKOWLEDGEMENTS

The authors thank Ross (Guanshen) Cui for protein preparations, Fiona Diffin and Alice Sears for assistance with DNA cloning, Dominik Kauert for advice on programming and Andreas Dahl for helpful discussions.

FUNDING

The Wellcome Trust (084086 to M.D.S.), the EU Marie Curie Research Training Network 'DNA Enzymes' (MRTN-CT-2005-019566 to M.D.S.), the Deutsche Forschungsgemeinschaft (DFG, SE 1646/1-1 and SE 1646/2-1 to R.S.) and the Dresden International Graduate School for Biomedicine and Bioengineering, funded by the DFG (to F.W.S.). Funding for open access charge: Wellcome Trust Value in People Award.

Conflict of interest statement. None declared.

REFERENCES

1. Szczelkun,M.D., Friedhoff,P. and Seidel,R. (2010) Maintaining a sense of direction during long-range communication on DNA. *Biochem. Soc. Trans.*, **38**, 404–409.
2. Meisel,A., Bickle,T.A., Kruger,D.H. and Schroeder,C. (1992) Type III restriction enzymes need two inversely oriented recognition sites for DNA cleavage. *Nature*, **355**, 467–469.
3. Meisel,A., Mackeldanz,P., Bickle,T.A., Kruger,D.H. and Schroeder,C. (1995) Type III restriction endonucleases translocate DNA in a reaction driven by recognition site-specific ATP hydrolysis. *EMBO J.*, **14**, 2958–2966.
4. Peakman,L.J., Antognozzi,M., Bickle,T.A., Janscak,P. and Szczelkun,M.D. (2003) S-Adenosyl methionine prevents promiscuous DNA cleavage by the EcoP1I type III restriction enzyme. *J. Mol. Biol.*, **333**, 321–335.
5. van Aelst,K., Toth,J., Ramanathan,S.P., Schwarz,F.W., Seidel,R. and Szczelkun,M.D. (2010) Type III restriction enzymes cleave DNA by long-range interaction between sites in both head-to-head and tail-to-tail inverted repeat. *Proc. Natl Acad. Sci. USA*, **107**, 9123–9128.
6. Peakman,L.J. and Szczelkun,M.D. (2004) DNA communications by Type III restriction endonucleases - confirmation of 1D translocation over 3D looping. *Nucleic Acids Res.*, **32**, 4166–4174.
7. Peakman,L.J. and Szczelkun,M.D. (2009) S-Adenosyl homocysteine and DNA ends stimulate promiscuous nuclease activities in the Type III restriction endonuclease EcoPI. *Nucleic Acids Res.*, **37**, 3934–3945.
8. Meisel,A., Kruger,D.H. and Bickle,T.A. (1991) M.EcoP15I methylates the second adenine in its recognition sequence. *Nucleic Acids Res.*, **19**, 3997.
9. Bachi,B., Reiser,J. and Pirrotta,V. (1979) Methylation and cleavage sequences of the EcoP1 restriction-modification enzyme. *J. Mol. Biol.*, **128**, 143–163.
10. Sears,A., Peakman,L.J., Wilson,G.G. and Szczelkun,M.D. (2005) Characterization of the Type III restriction endonuclease PstII from Providencia stuartii. *Nucleic Acids Res.*, **33**, 4775–4787.
11. Raghavendra,N.K. and Rao,D.N. (2004) Unidirectional translocation from recognition site and a necessary interaction with DNA end for cleavage by Type III restriction enzyme. *Nucleic Acids Res.*, **32**, 5703–5711.
12. Crampton,N., Roes,S., Dryden,D.T., Rao,D.N., Edwardson,J.M. and Henderson,R.M. (2007) DNA looping and translocation provide an optimal cleavage mechanism for the type III restriction enzymes. *EMBO J.*, **26**, 3815–3825.
13. Crampton,N., Yokokawa,M., Dryden,D.T.F., Edwardson,J., Michael,R., Desirazu,N., Takeyasu,K., Yoshimura,S.H. and Henderson,R.M. (2007) Fast-scan atomic force microscopy reveals that the type III restriction enzyme EcoP15I is capable

of DNA translocation and looping. *Proc. Natl Acad. Sci. USA*, **104**, 12755–12760.
14. Murray,N.E. (2000) Type I restriction systems: sophisticated molecular machines. *Microbiol. Mol. Biol. Rev.*, **64**, 412–434.
15. Seidel,R., van Noort,J., van der Scheer,C., Bloom,J.G.P., Dekker,N.H., Dutta,C.F., Blundell,A., Robinson,T., Firman,K. and Dekker,C. (2004) Real-time observation of DNA translocation by the type I restriction modification enzyme EcoR124I. *Nat. Struct. Mol. Biol.*, **11**, 838–843.
16. Stanley,L.K., Seidel,R., van der Scheer,C., Dekker,N.H., Szczelkun,M.D. and Dekker,C. (2006) When a helicase is not a helicase: dsDNA tracking by the motor protein EcoR124l. *EMBO J.*, **25**, 2230–2239.
17. Seidel,R., Bloom,J.G., Dekker,C. and Szczelkun,M.D. (2008) Motor step size and ATP coupling efficiency of the dsDNA translocase EcoR124I. *EMBO J.*, **27**, 1388–1398.
18. Saha,S. and Rao,D.N. (1995) ATP hydrolysis is required for DNA cleavage by EcoPI restriction enzyme. *J. Mol. Biol.*, **247**, 559–567.
19. Ramanathan,S.P., van Aelst,K., Sears,A., Peakman,L.J., Diffin,F.M., Szczelkun,M.D. and Seidel,R. (2009) Type III restriction enzymes communicate in 1D without looping between their target sites. *Proc. Natl Acad. Sci. USA*, **106**, 1748–1753.
20. Dryden,D.T., Edwardson,J.M. and Henderson,R.M. (2011) DNA translocation by type III restriction enzymes: a comparison of current models of their operation derived from ensemble and single-molecule measurements. *Nucleic Acids Res.*, **39**, 4525–4531.
21. Moncke-Buchner,E., Rothenberg,M., Reich,S., Wagenfuhr,K., Matsumura,H., Terauchi,R., Kruger,D.H. and Reuter,M. (2009) Functional characterization and modulation of the DNA cleavage efficiency of type III restriction endonuclease EcoP15I in its interaction with two sites in the DNA target. *J. Mol. Biol.*, **387**, 1309–1319.
22. Taylor,L.A. and Rose,R.E. (1988) A correction in the nucleotide sequence of the Tn903 kanamycin resistance determinant in pUC4K. *Nucleic Acids Res*, **16**, 358.
23. Vipond,I.B., Baldwin,G.S., Oram,M., Erskine,S.G., Wentzell,L.M., Szczelkun,M.D., Nobbs,T.J. and Halford,S.E. (1995) A general assay for restriction endonucleases and other DNA-modifying enzymes with plasmid substrates. *Mol. Biotechnol.*, **4**, 259–268.
24. Kunz,A., Mackeldanz,P., Mucke,M., Meisel,A., Reuter,M., Schroeder,C. and Kruger,D.H. (1998) Mutual activation of two restriction endonucleases: interaction of EcoPI and EcoP15. *Biol. Chem.*, **379**, 617–620.
25. Janscak,P., Sandmeier,U., Szczelkun,M.D. and Bickle,T.A. (2001) Subunit assembly and mode of DNA cleavage of the type III restriction endonucleases EcoP1I and EcoP15I. *J. Mol. Biol.*, **306**, 417–431.
26. Blainey,P.C., Luo,G., Kou,S.C., Mangel,W.F., Verdine,G.L., Bagchi,B. and Xie,X.S. (2009) Nonspecifically bound proteins spin while diffusing along DNA. *Nat. Struct. Mol. Biol.*, **16**, 1224–1229.
27. Bonnet,I., Biebricher,A., Porte,P.L., Loverdo,C., Benichou,O., Voituriez,R., Escude,C., Wende,W., Pingoud,A. and Desbiolles,P. (2008) Sliding and jumping of single EcoRV restriction enzymes on non-cognate DNA. *Nucleic Acids Res.*, **36**, 4118–4127.
28. Kingston,I.J., Gormley,N.A. and Halford,S.E. (2003) DNA supercoiling enables the Type IIS restriction enzyme BspMI to recognize the relative orientation of two DNA sequences. *Nucleic Acids Res.*, **31**, 5221–5228.
29. Watson,M.A., Gowers,D.M. and Halford,S.E. (2000) Alternative geometries of DNA looping: an analysis using the SfiI endonuclease. *J. Mol. Biol.*, **298**, 461–475.
30. Mizuuchi,K. (1992) Transpositional recombination: mechanistic insights from studies of mu and other elements. *Annu. Rev. Biochem.*, **61**, 1011–1051.
31. Stark,W.M., Boocock,M.R. and Sherratt,D.J. (1992) Catalysis by site-specific recombinases. *Trends Genet.*, **8**, 432–439.
32. Grindley,N.D., Whiteson,K.L. and Rice,P.A. (2006) Mechanisms of site-specific recombination. *Annu. Rev. Biochem.*, **75**, 567–605.
33. Janscak,P. and Bickle,T.A. (2000) DNA supercoiling during ATP-dependent DNA translocation by the type I restriction enzyme EcoAI. *J. Mol. Biol.*, **295**, 1089–1099.
34. Szczelkun,M.D. and Halford,S.E. (1996) Recombination by resolvase to analyse DNA communications by the SfiI restriction endonuclease. *EMBO J.*, **15**, 1460–1469.
35. Milsom,S.E., Halford,S.E., Embleton,M.L. and Szczelkun,M.D. (2001) Analysis of DNA looping interactions by type II restriction enzymes that require two copies of their recognition sites. *J. Mol. Biol.*, **311**, 515–527.
36. Embleton,M.L., Vologodskii,A.V. and Halford,S.E. (2004) Dynamics of DNA loop capture by the Sfil restriction endonuclease on supercoiled and relaxed DNA. *J. Mol. Biol.*, **339**, 53–66.
37. Wood,K.M., Daniels,L.E. and Halford,S.E. (2005) Long-range communications between DNA sites by the dimeric restriction endonuclease SgrAl. *J. Mol. Biol.*, **350**, 240–253.
38. Marshall,J.J., Gowers,D.M. and Halford,S.E. (2007) Restriction endonucleases that bridge and excise two recognition sites from DNA. *J. Mol. Biol.*, **367**, 419–431.
39. van den Broek,B., Lomholt,M.A., Kalisch,S.M., Metzler,R. and Wuite,G.J. (2008) How DNA coiling enhances target localization by proteins. *Proc. Natl Acad. Sci. USA*, **105**, 15738–15742.
40. Gemmen,G.J., Millin,R. and Smith,D.E. (2006) DNA looping by two-site restriction endonucleases: heterogeneous probability distributions for loop size and unbinding force. *Nucleic Acids Res.*, **34**, 2864–2877.
41. Gemmen,G.J., Millin,R. and Smith,D.E. (2006) Tension-dependent DNA cleavage by restriction endonucleases: Two-site enzymes are 'switched off' at low force. *Proc. Natl Acad. Sci. USA*, **103**, 11555–11560.
42. Fullwood,M.J., Wei,C.L., Liu,E.T. and Ruan,Y. (2009) Next-generation DNA sequencing of paired-end tags (PET) for transcriptome and genome analyses. *Genome Res.*, **19**, 521–532.